USE OF GEOSYNTHETICS TO MITIGATE EARTHQUAKE FAULT RUPTURE PROPAGATION THROUGH COMPACTED FILL

J. D. BRAY
A. ASHMAWY
PURDUE UNIVERSITY, USA

G. MUKHOPADHYAY
E. M. GATH
LEIGHTON AND ASSOCIATES, USA

1282

Eldon M. Gath, CEG
Principal Consultant
President

(714) 282-6122
FAX (714) 998-0971
Mobile (714) 412-2653

Earth Consultants International

2522 N. Santiago, Suite B
Orange, California 92867

Email: gath@worldnet.att.net
www.earthconsultants.com

ABSTRACT

A development project includes structures located in a zone containing minor subsidiary faults on the hanging wall of a potentially active thrust fault. Minor amounts of displacement on these subsidiary faults are possible. Previous studies suggest that differential movement across bedrock faults dissipates as the shear rupture plane rises through the overlying fills. The cost of extensive excavation and fill operations, however, may be prohibitive. Hence, the use of fill-reinforcement materials within smaller thicknesses of compacted fill was explored. In this paper, the project and site geology are described, the significant hazards associated with earthquake fault rupture are identified, and the finite element analyses are discussed. The numerical results indicate that the geosynthetic reinforcement is effective in spreading the differential movement across a wider zone. Differential settlement and tensile strains at the depth of the shallow foundations were reduced sufficiently to feasibly construct buildings with acceptable levels of risk at this site.

INTRODUCTION

A mixed use development project is under construction at a 250-acre site located on an anticlinal structure known as the Las Posas Hills in Camarillo, California. The Las Posas anticline is the surface expression of folding and thrusting along the Springville fault zone, a reverse fault system that is located immediately south of the project site. Geologic investigations discovered several extensional normal faults (axial faults) at the Las Posas anticline site. A number of these faults where old soil horizons were present were judged to be inactive. Many of these faults, however, do not have any overlying preserved soil units. In addition, the formational boundaries of the soil profiles are irregular, preventing the measurement of possible fault movements with a resolution level better than 2 to 5 cm. Hence, fault displacements on the order of 2 to 5 cm cannot be precluded for these axial faults. Therefore, the feasibility of attenuating (absorbing) minor fault displacements beneath the future structures at this site was explored.

Previous studies (Asquith and Leighton 1973; Bray et al. 1990) suggest that the differential movement of the underlying bedrock fault dissipates as the shear rupture plane propagates through the overlying compacted fill materials. If the depth of fill is sufficiently large and the underlying fault displacement is relatively small, the

Bray, J.D., Ashmawy, A., Mukhopadhyay, G., and Gath, E.M., 1993, Use of geosynthetics to mitigate earthquake fault rupture propagation through compacted fill; in Geosynthetics '93 Conference Proceedings, Industrial Fabrics Association International, St. Paul, MN, v.1, p. 379-392.

differential displacement of the underlying fault can be "locally absorbed" within the overlying fill. At this site, however, the costs associated with the extensive excavation and fill operations required to mitigate the hazardous effects at the ground surface could prove to be prohibitive. Hence, the use of fill-reinforcement materials was explored to optimize the depth of overexcavation and fill placement.

THE PROPOSED DEVELOPMENT AND PROJECT SITE DESCRIPTIONS

Proposed Development. The project involves balanced cut and fill grading to produce a series of acre-size residential lots, several multi-acre lots for commercial and high density residential use, an 18-hole golf course, and access roads. A schematic diagram of the proposed development and the faults is shown in Figure 1. Approximately twelve million cubic meters of cut and fill will be required to achieve the finish grade. The final graded site will be a series of natural, cut, fill and composite lots, terraced up from the perimeter lowlands to the centrally positioned ridge top. Terraced levels of the site will be separated by slopes of varying heights.

Maximum topographic relief at the site is roughly 90 m, with elevations ranging from 30 m at the property's west side to a maximum elevation of 120 m at the central ridge top. Natural slope gradients are between 4:1 and 2.5:1 (horz. to vert.) and appear to be controlled (to a degree) by the underlying geologic structure. No surface water was noted on the site. Ground water was encountered at a depth of about 12 m in several borings located along the property's perimeter.

Geology of the Las Posas Anticline. The Las Posas anticline and Springville thrust fault system is one of the several east-west trending fold and fault systems that have formed as a result of northeast compression and crustal shortening of the transverse ranges in southern California (Yerkes and Lee 1979). The Las Posas Hills are underlain by fine-grained siltstone, sandstone and several associated paleosols assigned to the Saugus formation. This formation is estimated to be 200 to 600 thousand years old (Rockwell et al. 1985). At the crest of the anticline, these fine-grained deposits are locally overlain by a coarser grained, gravelly alluvial deposit that is estimated to be about 120 thousand years old, and a finer grained colluvial soil with a minimum development age of approximately 15 thousand years (Leighton and Associates 1991). The gravelly sediments at the crest of the anticline were deposited as stream channel deposits by a precursor stream to the modern Santa Clara river at about the same time, or just prior to the hills starting to be uplifted. This suggests that folding and growth of the anticline began no more than 120 thousand years ago. Initially, the anticline grew primarily as a result of folding, with minor compression along a buried (or "blind") thrust fault that developed into the modern Springville fault. The Springville fault is estimated to have broken through to the surface as recently as 15 to 30 thousand years ago. Since then, the hills are growing primarily by thrusting along the Springville fault. Once the blind thrust fault became a surface fault, folding and deformation of the Las Posas anticline was replaced by passive uplift.

Two types of secondary faulting have been observed at the crest of the anticline; namely, east-west trending normal bending moment faults (axial) and north-south trending tear faults (Gath and Whitney 1992). The axial faults formed by extension of the sediments during the time period when the anticline was growing primarily as a result of folding (see Figure 1). Episodic displacements on the axial faults could have also occurred with a movement pattern typical of a normal fault during the seismic events on the blind Springville fault. Formation of the tear faults is associated with the Springville fault having broken through to the surface at different times along the different portions of the anticline. Thus, while some sections of the hill were being

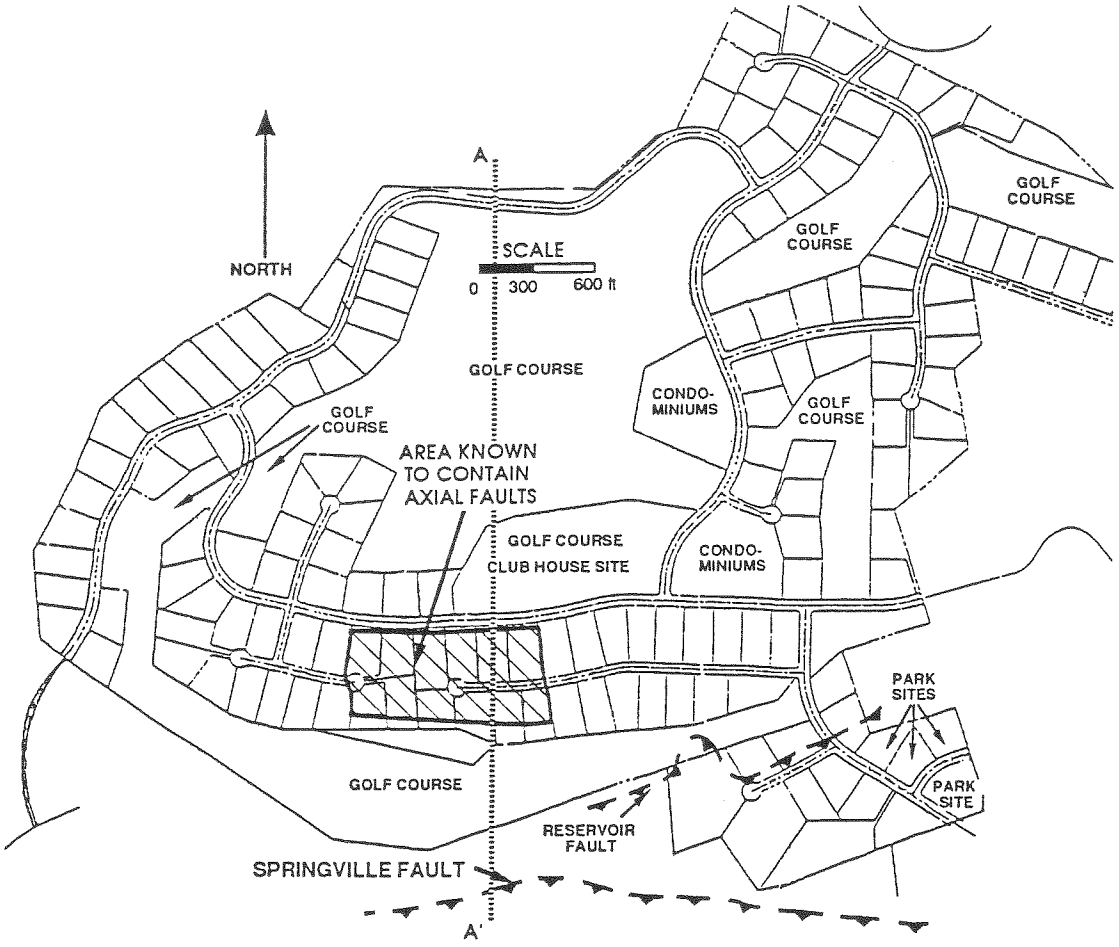

(a) Plan view of the proposed development showing the fault locations.

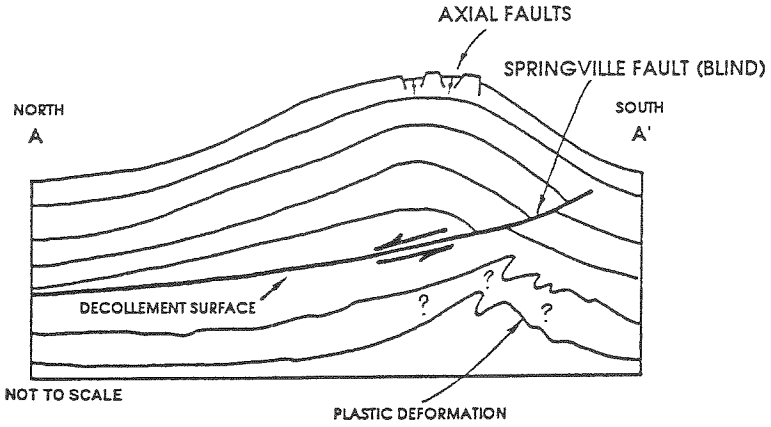

(b) Generalized cross-section A-A' showing the axial faults formed when the Springville fault was a blind structure.

Figure 1. Schematic diagram of the proposed development showing the relationship between the Springville thrust fault and the axial faults at the crest of the Las Posas anticline

uplifted primarily by folding, other sections were growing primarily by faulting. Tear faults formed at the margins between these two types of anticlinal growth. Since the Springville fault surfaced, the axial and tear faults have presumably been deactivated, or have been reactivated only coseismically with the movement on the Springville fault. The axial and tear faults themselves are not believed to be seismologically active.

Magnitude and Probability of Axial Fault Displacement. Preliminary results, based on radiocarbon dating of charcoal samples collected in a trench where the Springville fault was exposed, suggest that an event on the Springville fault occurred as recently as 1,000 years ago. A similar magnitude event (based on a similar amount of displacement) occurred about 3,000 to 5,000 years earlier, suggesting that the Springville fault has a recurrence interval of about 3,000 to 5,000 years. The axial and tear faults extend into, and offset the gravelly deposits that are estimated to be 120,000 years old, but they do not appear to affect the 15,000 year-old soils. Because the soil horizons have irregular and gradual lower boundaries, individual displacements on these faults of about 5 cm or less cannot be precluded. The recurrence interval of 3,000 years for the Springville fault suggests that about five earthquakes have occurred on this system in the last 15,000 years. One could interpret that the fault displacements, if any, on the axial and tear faults have occurred during these events, to produce a maximum total displacement of 5 cm.

The probability of occurrence of earthquakes is often estimated based on the Poisson's distribution model:

$$P\ (\text{Occurrence}/T,N) = 1-e^{-T/N} = 1-(1-1/T)^{N} \qquad (1)$$

where:
T = the recurrence interval in years;
N = the design life in years.

The term 1/T could be interpreted as the annual risk for the occurrence of an earthquake. Equation (1) could also be used to estimate the displacement if the annual risk for observing the displacement at the site is known. The probability of occurrence of 1, 2.5, and 5 cm displacement on the axial faults at the site were estimated based on these assumptions: (1) Each of the five past significant earthquake event caused the same amount of displacement. Hence, each future earthquake will cause 1 cm of displacement with no uncertainty involved; (2) Only two past earthquakes caused the 5 cm displacement. Hence, the chance of observing 2.5 cm displacement due to a future earthquake is about 2 out of 5; and (3) Only one past earthquake caused the 5 cm displacement. Hence, the chance of observing 5 cm displacement due to a future earthquake is about 1 out of 5. The probability of occurrence of these magnitudes of fault displacement in a 100-year period at the site based on 3,000-year return period for a seismic event on the Springville fault are shown in Table 1.

HAZARDS ASSOCIATED WITH EARTHQUAKE FAULT RUPTURE PROPAGATION THROUGH COMPACTED FILL

Earthquake Fault Rupture. A number of geologists have found that the principal factors controlling the general characteristics of surface faulting are: (a) the type of fault movement (reverse, normal, or strike-slip), (b) the inclination of the fault plane, (c) the amount of displacement on the fault, (d) the depth and geometry of the earth materials overlying the bedrock fault, and (e) the nature of the overlying earth materials (e.g. Bonilla 1988). Two examples which illustrate characteristics of fault rupture propagation through overlying soils are shown in Figures 2 and 3. Typically, reverse faults tend to gradually decrease in dip near the ground surface. Normal

Table 1. Probability of occurrence of axial fault displacement in a 100 year period[a]

Case	Fault Displacement (cm)	Annual Risk (%)	Probability of Occurrence
1	1.0	1/3000	3.0
2	2.5	1/3000 * 2/5	1.3
3	5.0	1/3000 * 1/5	0.7

[a] Based on 3,000 year return period for on the Springville fault

faults tend to refract at the soil-bedrock contact and increase in dip as they approach the ground surface. This refraction and variation of the dip of the normal fault plane may produce gravity grabens. Strike-slip faults tend to follow the almost vertical orientation of the underlying bedrock fault, although the rupture zone may spread or "flower" near the ground surface. Relative motion is primarily concentrated within a relatively narrow zone above the bedrock fault. Once failure occurs, differential movement is usually localized to thin, distinct failure planes. Ductile materials, however, may accommodate significant fault movement by warping without actually developing distinct shear surfaces.

Geologic field studies at the project site suggest that the bedrock faults are principally either normal faults dipping between 45 and 60 degrees or nearly vertical strike-slip faults. Most of these fault features are exposed or will be exposed during grading operations. Hence, overexcavation will be required to construct compacted fill over the bedrock faults to mitigate the surficial hazards associated with base rock fault displacements. The depth of overexcavation should be minimized, however, to control costs and to reduce the potentially deleterious effects of the other more routine design considerations (e.g. shrink/swell/collapse under static service loads). The results of previous investigations (Bray et al. 1990) suggest that dip-slip fault movements (especially normal faults which induce extensional strains within the overlying soil) pose a greater hazard than strike-slip fault movements. Hence, two-dimensional (2-D) finite element (FE) analyses of dip-slip base rock axial fault displacements will be investigated. For the purpose of this study, movement on a normal fault plane dipping at 60 degrees has been considered as the baseline case.

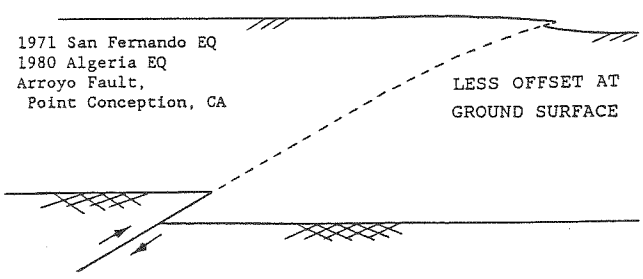

Figure 2. Path of "shallow" reverse fault rupture through "stiff" soils

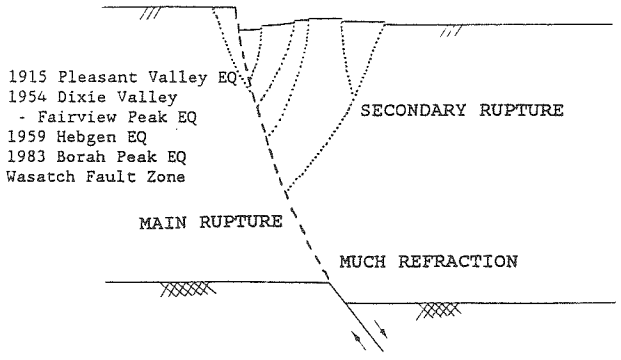

Figure 3. Path of "shallow" normal fault rupture through "stiff" soils

Hazards. The principal surficial hazards of base rock fault displacements are:

(A) propagation of the distinct shear rupture plane to the ground surface,
(B) differential settlement or angular distortion of the ground surface,
(C) compressive or tensile horizontal strains at the ground surface, and
(D) development of surficial tension cracks.

Of course, the earthquake event that produces the relative movement on these subsidiary fault features will also produce strong shaking. This study focuses on the response of the compacted fill to base rock fault displacements and has not considered the potential for building damage due to earthquake strong shaking.

Performance Criteria. Based on an evaluation of the seismicity of the Springville fault and the probable range of displacements on the axial faults, the project's grading specifications were developed based on the 2.5 cm axial fault displacement. The probability of occurrence of the 2.5 cm axial fault displacement was estimated to be 1.3 percent (see Table 1). Conceptually, this risk level is more stringent than the seismic risk level stipulated by the 1991 California Building Code for the design of essential facilities such as hospitals. This degree of conservatism, however, was considered warranted because of the recency of the discovery of the Springville fault, the uncertainty in the profession's understanding of earthquake fault rupture, and the perceived sensitivity of the potential homeowners to this problem.

Regarding the principal hazards of base rock fault displacements described previously, the project's performance criteria at the 2.5 cm magnitude of fault offset follows. Propagation of the rupture plane to the ground surface was considered unacceptable (Hazard A). The angular distortion over a reasonable length (3 m) should be less than 1/400 (Hazard B). Since post-tensioned foundation slabs were being recommended, this conforms to standard practice in southern California. Based on accepted mining subsidence practices and appropriate foundation design provisions, horizontal tensile strains in the soil were to remain less than 0.3 percent (Hazard C) and tensile stresses at the ground surface were not to exceed 1 kPa.

FINITE ELEMENT ANALYSIS OF EARTHQUAKE FAULT RUPTURE PROPAGATION

Finite Element Procedures. Previous numerical studies of fault rupture propagation through earth materials suggest that the FE method can be applied to this class of problems provided an incremental nonlinear stress-strain soil behavior model is employed (Bray et al. 1990). The plane strain FE computer program SSCOMPPC (Boulanger et al. 1991), which employs a hybrid incremental load solution technique with the Duncan et al. (1980) hyperbolic soil behavior model, was utilized in this study to model the nonlinear stress-dependent stress-strain and volumetric strain behavior exhibited by typical compacted soils. The principal advantages of this particular numerical approach are its relative simplicity and its ability to adequately model the soil's failure strain. The well-validated FE program SSCOMPPC also allows discrete modelling of the soil, the reinforcement, and the soil-reinforcement interface.

Development of Model Parameters. A series of triaxial compression tests were performed on three bulk samples believed to be representative of the fill materials to be used on the project site (USCS soil classifications: SM-SC, ML and SW-SM). Anisotropically consolidated undrained triaxial compression tests (CAU) were performed on all three fill materials at 90% or 95% relative compaction (RC) and at optimum, optimum +3% and optimum +5% moisture contents (MC) with respect to the ASTM 1557 maximum dry density and optimum moisture content. The test specimens were consolidated to stress states

Table 2. Hyperbolic soil model parameters employed to represent baseline soil

Case	Clayey Silty Sand Soil (SM-SC)	ϵ_f (%)	c (kPa)	ϕ (deg)	K	n	R_f	γ (Mg/m^3)
A	MC = Opt+5% & RC = 90%	3-6	36	33	800	1.0	0.95	2.07
B	MC = Opt+3% & RC = 95%	2-3	29	40	600	0.8	0.7	2.15
C	MC = Opt & RC = 90%	4-8	48	28	900	1.0	0.98	1.94
$\Delta\phi = 0$; $K_{ur} = 1.5$ K; $K_b = 1.5$ K and m = n so that $\upsilon_i \approx 0.4$								

representative of field condition (K_o=0.6), and the strain rate during undrained shear was deliberately high (125%/hr) to simulate at least qualitatively the high strain rates imposed by an earthquake base rock fault displacement.

The stress-strain behavior of the three fill materials at similar RC and relative MC did not differ appreciably. Since the clayey silty sand materials (SM-SC) was judged to be a mix of the predominant materials on site, it constitutes the baseline soil. In addition to the CAU tests, isotropically consolidated drained tests (CID) and undrained tests (CIU) were performed on the baseline soil at slower strain rates to evaluate the volume change behavior and pore pressure response of the soil during loading. These tests also investigated possible strength loss upon saturation of the compacted fill materials. The CID and CIU tests indicated that the material exhibited contractive behavior during shear at the densities and confining pressures representative of field conditions. Based on these test results and previous experience with similar partially saturated compacted fill materials, the initial magnitude of Poisson's ratio was assumed to be within the range of 0.35 to 0.45. As undrained shear progresses, Poisson's ratio will tend to increase.

Duncan et al. (1980) hyperbolic soil model parameters were developed for each test series, and the model parameters for the baseline soil (SM-SC) are presented in Table 2. The hyperbolic model representation of the stress-strain behavior of the Case A compacted fill test series is shown in Fig. 4. In general, the model represented the compacted fill's behavior well. Due in part because of the high strain rates imposed

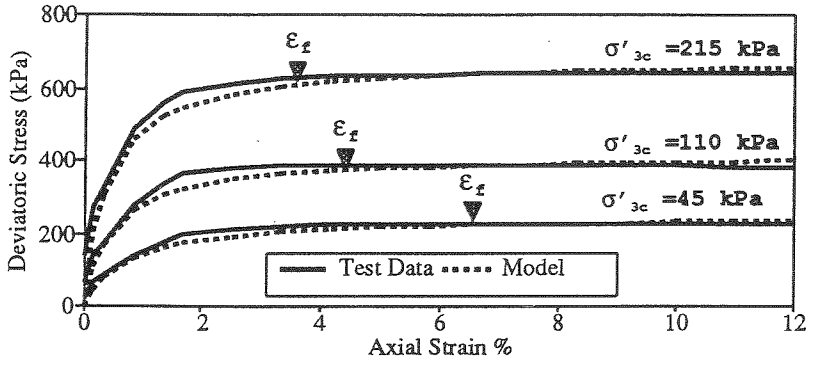

Figure 4. Hyperbolic model's representation of the baseline material (SM-SC) compacted at MC = opt+5% and RC = 90% (Case A)

Table 3. Results of FE analyses of unreinforced compacted fill

Description	Fill Ht. (m)	Base Fault Offset (cm)	HAZARD A Ht. of Shear Zone above bedrock (m)	HAZARD B Angular Distortion over 3m zone (δ/L)	HAZARD C Max. Tensile Strain at Surface (%)	HAZARD D Max. Tensile Stress at Surface (kPa)
SM-SC (Case A) RC=90%, MC=+5%	4.5	2.5	<1.0	1/180	0.6	2.9
		5.0	<1.5	1/85	1.0	7.2
	6.0	2.5	<1.0	1/220	0.4	1.2
		5.0	<1.5	1/100	1.0	4.8
	9.0	2.5	<1.0	1/300	0.25	0.5
		5.0	<1.5	1/130	0.5	2.4
	12.0	2.5	<1.0	1/400	0.2	None
		5.0	<1.5	1/175	0.4	1.2
SM-SC (Case A) over 2m of CL	6.0	2.5	<0.3	1/250	0.3	1.1
		5.0	<0.5	1/115	0.5	2.4
SM-SC (Case B) RC=95%, MC=+3%	6.0	2.5	<1.0	1/230	0.4	3.1
		5.0	<2.5	1/110	1.0	4.8
SM-SC (Case C) RC=90%, MC=+0%	6.0	2.5	<1.0	1/220	0.6	3.6
		5.0	<1.5	1/100	1.0	9.6
ML RC=90%, MC=+5%	6.0	2.5	<1.0	1/220	0.3	12.0
		5.0	<2.0	1/100	0.75	24.0
SW-SM RC=90%, MC=+5%	6.0	2.5	<1.5	1/200	0.4	14.0
		5.0	<4.5	1/100	1.0	17.0

during shear, these model parameters display fairly stiff stress-strain behavior (i.e. high modulus numbers, K) with respect to model parameters typically used in design (Duncan et al. 1980). Multiple analyses were performed to note the sensitivity of the results to slight variations in the soil model parameters developed to represent the soil's nonlinear stress-dependent behavior.

PERFORMANCE OF UNREINFORCED FILL

Representative results of the FE analysis of the unreinforced compacted fill are summarized in Table 3. The deformed FE mesh shown in Figure 5 illustrates the deformation pattern that developed in a 6 m high compacted fill overlying a 60° normal fault displacement of 2.5 cm. The development of the shear rupture plane within the compacted fill for this condition is shown in Figure 6. For this case, the differential movement across the distinct bedrock fault plane is locally "absorbed" within the overlying compacted fill (Hazard A). The distinct bedrock fault offset is spread out over a wider zone of general shear at the ground surface. Because of the

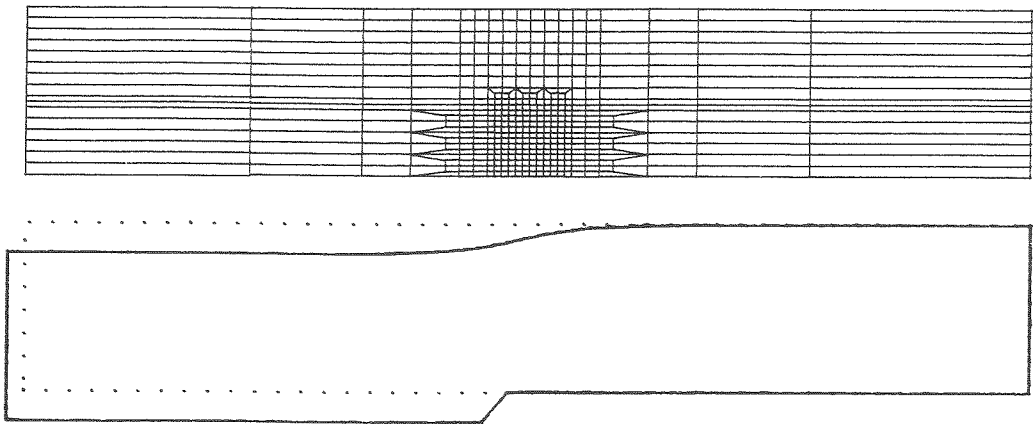

Figure 5. FE mesh and deformed mesh outline for 6m high compacted fill (SM-SC, Case A) and 2.5 cm base fault offset (displacements magnified by 50)

compacted fill soil's relatively stiff stress-strain response, however, the majority of differential movement (≈75%) occurs within a fairly narrow zone (≈3 m) along the projection of the base rock fault. The angular distortion across this 3 m wide zone is on the order of 1/220 for the 2.5 cm base rock fault offset (Hazard B). This magnitude of angular distortion can produce structural damage in some of the building's components, however, collapse is unlikely. The fill height must be increased to 12 m to reduce the angular distortion across a 3 m wide zone to roughly 1/400. The maximum tensile strain for the 6 m high unreinforced fill is 0.4% although the average horizontal tensile strains across a reasonable length (3 m) is less than 0.2% (Hazard C). It is unlikely that (and in fact the foundation can be modified so that) the full horizontal strain developed in the soil below the foundation is not transferred to the structural foundation. Finally, zones at the ground surface where the minor principal stress is negative are not extensive for this case (Hazard D).

As shown in Table 3, the FE results suggest that as the fill height increases or the design base rock fault displacement decreases, the hazards associated with earthquake fault rupture are minimized. For a given fill height and magnitude of fault

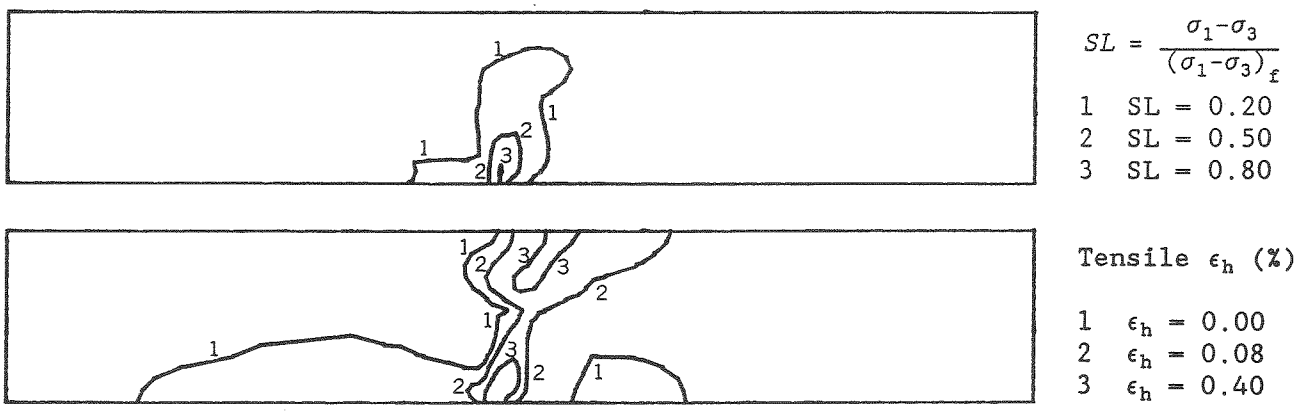

Figure 6. Stress level (SL) contours and horizontal strains for 6 m high compacted fill (SM-SC, Case A) and 2.5 cm base fault offset

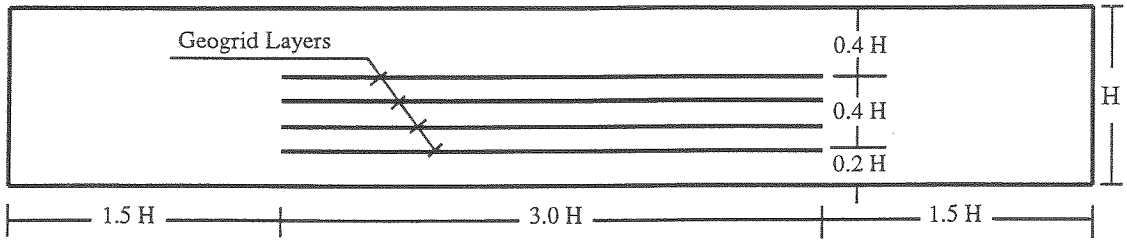

Figure 7. Location of reinforcement layers in compacted fill

offset, the earthquake fault rupture hazards are reduced as the ductility of the compacted fill increases. For example, the placement of a 2 m thick "ductile" low-plasticity clayey material (CL) directly above the bedrock fault significantly improves the performance of the fill with respect to earthquake fault rupture. The FE results also suggest that the baseline soil (SM-SC) should be compacted wet of optimum and at the lower range of acceptable dry densities. Kneading compaction should be specified to further increase the ductility of the compacted fill.

Given the project's performance criteria for the 2.5 cm bedrock fault offset, the unreinforced fill height would have to be 12 m high. This fill height requires extensive overexcavating and is considered prohibitive in terms of cost and time.

PERFORMANCE OF REINFORCED FILL

The FE mesh was modified as shown in Figure 7 to include up to four layers of reinforcement. The FE program SSCOMPPC modelled the Tensar UX1500 geogrid (EA=890kN, Ultimate Strength=86kN/m) as linear elastic bar elements that sustained only tensile forces and the soil-geogrid interface as a nonlinear stress-dependent zero thickness element that controlled the relative displacement of adjacent soil and structural element nodal points (Clough and Duncan 1969). The hyperbolic model parameters selected to model the soil-geogrid interface were based on a soil-geogrid interaction coefficient of 0.9 (i.e. c = 18 kPa, ϕ = 30°, K_{ss} = 27130, R_f = 0.95, n = 1.0).

Representative results of the FE analysis of the reinforced compacted fill are summarized in Table 4. Examining the case where two geogrids are placed within a 6 m high compacted fill composed of the baseline soil and subjected to a 2.5 cm base rock fault displacement, the differential movement across the distinct bedrock fault plane is locally "absorbed" within the overlying compacted fill (Hazard A). The angular distortion over a 3 m wide zone along the projection of the bedrock fault plane is roughly 1/400 (Hazard B). The maximum tensile strain at the surface is 0.25% (Hazard C) and the tensile stresses at the surface are minimal (Hazard D). In all cases, the maximum tensile force developed in the geogrid remain less than its established ultimate tensile capacity (FS≈2 for the 5 cm bedrock fault offset).

Given the project's performance criteria for the 2.5 cm bedrock fault offset, the reinforced fill height would have to be 6 m high. This fill height requires minimal overexcavation and is acceptable in terms of cost and time. The additional cost of the two Tensar UX1500 geogrid in place is only about $15 per square meter in the areas containing identified subsidiary bedrock faults.

As Table 4 indicates, a number of analyses were performed under different conditions to investigate the sensitivity of the results to variations in the input

Table 4. Results of FE analyses of reinforced compacted fill

Description[a]	Base Fault Offset (cm)	HAZARD A Ht. of Shear Zone above bedrock (m)	HAZARD B Angular Distortion over 3m zone (δ/L)	HAZARD C Max. Tensile Strain at Surface (%)	HAZARD D Max. Tensile Stress at Surface (kPa)	Max. Geogrid Force (kN/m)
SM-SC (Case A) without reinf.	2.5	<1.0	1/220	0.4	1.2	--
	5.0	<1.5	1/100	1.0	4.8	--
SM-SC (Case A) with 2 geogrids	2.5	<1.0	1/400	0.25	0.2	22
	5.0	<1.5	1/200	0.5	2.4	44
2 geogrids 4.5m high fill	2.5	<1.0	1/310	0.3	1.3	25
	5.0	<1.5	1/170	0.6	3.6	48
2 geogrids 9.0m high fill	2.5	<1.0	1/670	0.15	None	17
	5.0	<2.0	1/280	0.3	0.7	35
2 geogrids interaction reduced 50%	2.5	<1.0	1/400	0.25	0.5	21
	5.0	<1.5	1/200	0.5	2.4	41
2 geogrids, geogrid EA reduced 90%	2.5	<1.0	1/450	0.25	0.5	3
	5.0	<1.5	1/240	0.5	2.9	6
4 geogrids	2.5	<1.0	1/425	0.2	0.3	27
	5.0	<1.5	1/200	0.4	1.9	42

[a] Results are for 6m high fill (SM-SC, Case A) except where noted.

parameters. Limiting angular distortion was the governing performance criteria for this project. Hence, figures which depict the deformed shape of the surface of the compacted fill overlying a 60° normal fault displacement of 2.5 cm will be examined.

As shown in Figure 8, the geogrid reinforcement is effective in spreading the differential movement, across the distinct bedrock fault across a wider zone of general shear in the fill. Hence, the angular distortion across a reasonable width (3 m) is greatly reduced with the use of the geosynthetic reinforcement. In these plane strain analyses, the FE model enforces uniform displacements at the left and right boundaries of the mesh as one would expect if the underlying bedrock in this area displaced uniformly. The reinforced compacted fill increases the width of the transition zone at the ground surface. Finally, the performance of the compacted fill reinforced with four layers of geogrid instead of two layers is only slightly better, and the improved performance is judged to be inconsequential.

As shown in Figure 9, increasing the reinforced fill height spreads the bedrock fault displacement across a wider zone of general shear in the fill. The results, however, appear to be insensitive to reductions in the soil-geogrid interaction

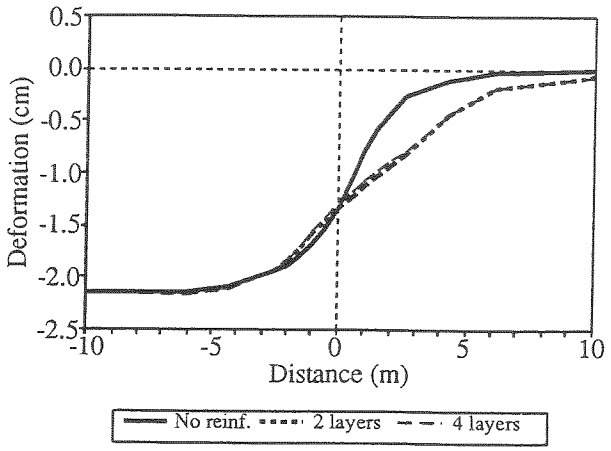

Figure 8. Effect of reinforcement to reduce differential movements at surface of 6 m high fill

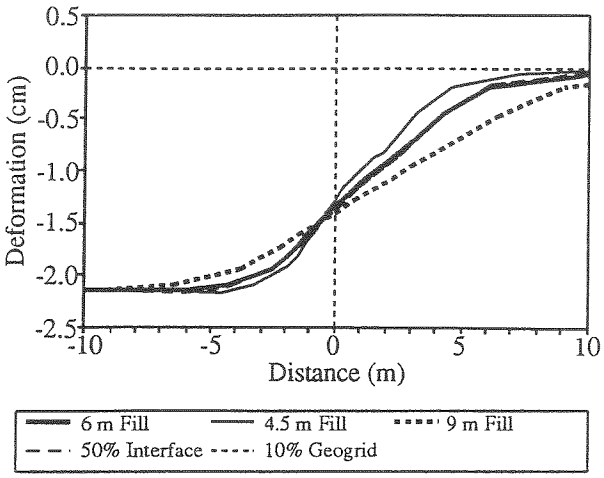

Figure 9. Effect of variations in the reinforced fill height, geogrid properties and interface properties

coefficient and the geogrid's stiffness. The stiffness of the reinforcement appears to be less important because it is relatively stiff compared to the soil. Although the magnitudes of angular distortion calculated by the FE analyses are fairly insensitive to the soil-geogrid interaction coefficient within the range of movements examined in this study, the FE results indicate a large number of failed soil-structure interface elements at the 5 cm magnitude of bedrock fault offset for the case with a 50% reduction in the soil-geogrid interaction coefficient. For this case, the reinforcement is beginning to lose its effectiveness at this level of movement. Hence, soil-reinforcement with the higher soil-geogrid interaction coefficients such as Tensar UX1500 should be used. Finally, the soil-reinforcement must possess adequate tensile capacity with a reasonable safety factor, and the FE results suggest that at least two layers of reinforcement are necessary within the compacted fill.

DISCUSSION OF RESULTS

The FE results suggest that there are principally three construction techniques effective in mitigating the potential hazards associated with earthquake base rock fault rupture propagation through compacted fill. The hazards can be reduced by: (1) increasing the ductility of the compacted fill, (2) increasing the height of the compacted fill, and (3) installing soil-reinforcement within the compacted fill.

On this project, large volumes of fill material were required, and hence it was impractical to not use on-site materials as fill. Laboratory test results indicated that the fill material was fairly stiff, but that ductility could be increased by placing the fill material wet of optimum at lower dry densities with kneading compaction. The performance of the compacted fill could be further enhanced by increasing its thickness. The FE results indicated that the unreinforced compacted fill would have to be 12 m high to meet the project's performance criteria for the 2.5 cm bedrock fault offset. This fill height required extensive overexcavating and was considered prohibitive in terms of additional cost and time.

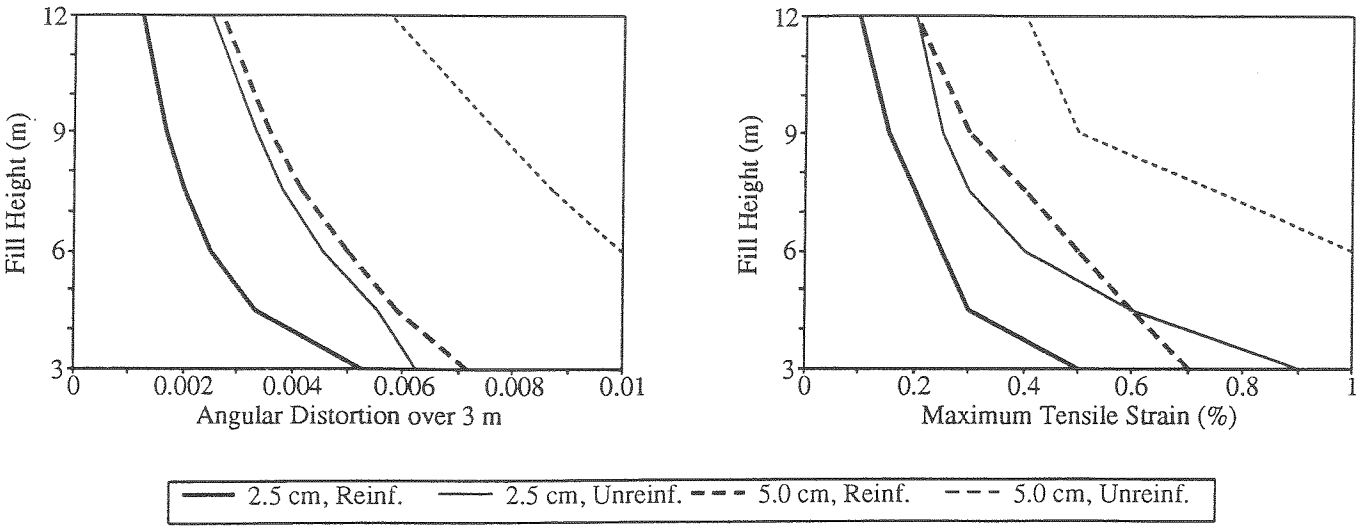

Figure 10. Comparison of unreinforced and reinforced compacted fill for baseline case (SM-SC, MC=opt+5%, RC=90%) for 2.5 cm and 5.0 cm fault offsets

The soil-reinforcement proved effective in spreading the differential movement across the bedrock fault across a wider zone of shear in the fill, thereby reducing the angular distortion (Hazard B), horizontal tensile strains (Hazard C), and the tensile stresses (Hazard D) at the ground surface. The height of the shear rupture zone in the compacted fill overlying the displaced bedrock fault (Hazard A) was insensitive to the use of soil-reinforcement, but this hazard did not govern the design.

The improved performance of the reinforced compacted fill is shown in Figure 10. In this figure, the angular distortion across a 3 m wide zone at the ground surface and the maximum tensile strain at the ground surface are plotted against the fill height for both the unreinforced and reinforced compacted fill subjected to 2.5 cm and 5.0 cm base rock fault offsets. The FE results indicate that the angular distortion (Hazard B) and the maximum tensile strain (Hazard C) is roughly inversely proportional to the fill height. In addition, these potential hazards are significantly reduced by including fill-reinforcement materials within the compacted fill. Specifically, to satisfy the project's performance criteria, a 6 m high reinforced compacted fill is required in lieu of a 12 m high unreinforced compacted fill. This improved performance is achieved by installing 2 layers of Tensar UX1500 geogrid within the bottom half of the fill. The findings of this FE study agree generally with the results of published laboratory tests which indicated that the geosynthetic reinforcement was effective in spreading differential movement in a direct shear apparatus across a wider zone of shear (Shewbridge and Sitar 1989).

CONCLUSIONS

Small amounts of displacement on minor subsidiary faults could produce structural damage in the buildings' shallow foundations at a development project in southern California. The results of this study as well as that of previous studies suggest, however, that differential movement across distinct bedrock faults dissipates as the shear rupture plane rises through overlying fills. At this site, the cost of extensive excavation and fill operations required to mitigate the hazards associated with earthquake fault rupture propagation in this manner proved to be prohibitive. Hence,

the use of fill-reinforcement materials within smaller thicknesses of compacted fill was explored. The FE results indicated that the soil-reinforcement was effective in spreading the differential movement across the distinct bedrock fault plane across a wider zone of shear in the reinforced compacted fill. This spreading of the localized base rock fault offset minimized the differential settlement and tensile strains at the depth of the buildings' shallow foundations making it feasible to construct buildings with acceptable levels or risk at this site.

ACKNOWLEDGEMENTS

Financial support was partially provided by the National Science Foundation under grant No. BCS-9157083. This support is gratefully acknowledged.

REFERENCES

Asquith, D.O., and Leighton, F.B. (1973) "Earth Rupture and Structural Damage by San Fernando Earthquake in North Sylmar Housing Development," In San Fernando, California Earthquake of February 9, 1971, U.S. Depart. of Commerce, Washington D.C., pp. 207-212.

Bonilla, M. G. (1988) "Minimum Earthquake Magnitude Associates with Coseismic Surface Faulting," Bull. Association of Engineering Geologists, Vol. XXV, No. 1, pp. 17-29.

Boulanger, R. W., Bray, J. D., Chew, S. H., Seed, R. B., Duncan, J. M., and Mitchell, J. K. (1991) "SSCOMPPC: A Finite Element Analyses Program for Geotechnical Analysis of Soil-Structure Interaction, Earth Dams, and Compaction Effects," Univ. of California, Berkeley Geotech. Engr. Report, UCB/GT/90-02, April.

Bray, J. D., Seed, R. B., and Seed, H. B. (1990) "The Effects of Tectonic Movements on Stresses and Deformations in Earth Embankments," Earthquake Engineering Research Center, Report No. UCB/EERC-90/13, July.

Clough, G. W., and Duncan, J. M. (1969) "Finite Element Analyses of Port Allen and Old River Locks," Univ. of California, Berkeley Geot. Engr. Report, TE-69-3, Sept.

Duncan, J. M., Byrne, P., Wong, K. S., and Mabry, P. (1980) "Strength, Stress-Strain and Bulk Modulus Parameters for Finite Element Analyses of Stresses and Movements in Soil Masses," Univ. of California, Berkeley Geot. Engr. Report, UCB/GT/80-01, Aug.

Gath, E.M., and Whitney, R.A. (1992) "Faulting and Tectonic Model of the Las Posas Anticline, Western Transverse Ranges, and Implications for Seismic Risk in the Ventura Basin Region, California", Amer. Assoc. of Petrl. Geol. Bull., Vol. 76, No. 3, pp. 419.

Leighton and Associates, Inc. (1991) "Axial Fault Study, Spanish Hills, Tract 4227, Phase II, City of Camarillo, California," Report to the Spanish Hills Development Company, dated June 13, 1991, Project No. 3901427-04.

Rockwell, T.K., Keller, E.A., and Dembroff, G.R. (1985) "Quaternary Rate of Folding of the Ventura Avenue Anticline, Western Transverse Ranges, Southern California," Geological Society of America Bull., Vol. 100, pp. 850-858.

Shewbridge, S.E., and Sitar, N. (1989) "Deformation Characteristics of Reinforced Sand in Direct Shear," J. of Geotechnical Engineering, ASCE, Vol. 115, No. 8, pp. 1134-1147.

Yerkes, R.F., and Lee, W.H.K. (1979) "Late Quaternary Deformation in the Western Transverse Ranges, California," U.S. Geological Survey Circular 799-B, pp. 27-37.